RESEARCH ARTICLE
doi: 10.2306/scienceasia1513-1874.2016.42.033

*ScienceAsia* 42 (2016): **33–39**

# The speed of reaction-diffusion fronts on fractals: testing the Campos-Méndez-Fort formula

**Orapun Suwannasen**[a], **Michael A. Allen**[b,*], **Julien Clinton Sprott**[c]

[a] Mathematics Department, Faculty of Science, Mahidol University, Rama 6 Road, Bangkok 10400 Thailand
[b] Physics Department, Faculty of Science, Mahidol University, Rama 6 Road, Bangkok 10400 Thailand
[c] Department of Physics, University of Wisconsin, Madison, WI 53706 USA

*Corresponding author, e-mail: maa5652@gmail.com

*Received 18 Sep 2015*
*Accepted 29 Feb 2016*

**ABSTRACT**: Campos, Méndez, and Fort (CMF) derived an approximate formula for the speed of reaction-diffusion fronts in fractal media. By way of a continuation of their earlier studies, we perform numerical simulations of reaction-diffusion equations with $au(1-u)(1-\alpha u)$ for $0 \leqslant \alpha \leqslant 1$ as the reaction term on various generalized Sierpiński carpets (including infinitely ramified and random ones). The CMF formula agrees well with the mean front speed as a function of $a$ obtained from our simulations for the classic Sierpiński carpet, a randomized version of the carpet, and some finitely ramified carpets containing loops. In these cases the mean front speed also shows no significant dependence on $\alpha$, as predicted by the CMF formula. However, the agreement is not so good in the case of the other carpets tested and this is probably a result of the mean distance of the front from the starting point against time behaving erratically in such cases. We also propose some nomenclature for generalized Sierpiński carpets and introduce a compact formulation of how to determine whether a point is on a generalized Sierpiński carpet lattice.

**KEYWORDS**: random walk dimension, generalized Sierpiński carpet, Fisher equation, subdiffusion

## INTRODUCTION

Reaction-diffusion equations with stable travelling wavefront solutions apply to such diverse systems as autocatalytic reactions[1] and a fairy ring of mushrooms[2]. Here we consider reaction-diffusion equations with one dependent (dimensionless) variable $u$ of the form

$$\frac{\partial u}{\partial t} = D\nabla^2 u + uf(u), \qquad f(1)=0, \quad \max_{0\leqslant u\leqslant 1} f(u) = f(0), \tag{1}$$

where $D$ is the diffusion coefficient. Eq. 1 with $f(u) = a(1-u)$, where $a$ is a positive constant, is known as the Fisher equation and was first proposed to model the spread of advantageous genes[3], but is now more familiar as an equation governing a population of organisms exhibiting logistic growth[4].

As fractal media are widespread in nature[5], how reaction-diffusion fronts propagate on fractals is of great interest. At the microscopic level, diffusion arises from particles performing random walks and these are governed by

$$\left\langle r^2 \right\rangle = Ct^{2/d_w}, \tag{2}$$

where $\left\langle r^2 \right\rangle$ is the mean squared displacement of the particles from their starting positions after time $t$, $d_w$ is the random walk dimension, and $C$ is a constant which depends on the size of the steps the particles take and the geometry of the medium. A description of diffusive processes on fractals should also agree asymptotically with the following probability, obtained in Ref. 6 by considering an intrinsic metric for fractals, of finding a particle at distance $r$ after time $t$:

$$P(r,t) \sim t^{-d_f/d_w} \exp\left[-c\left(\frac{r}{t^{1/d_w}}\right)^{1/\delta}\right], \tag{3}$$

where $d_f$ is the fractal dimension, $c$ is a constant, $\delta \equiv d_{\min}^{-1} - d_w^{-1}$, and $d_{\min}$ is the minimum distance dimension (see, e.g., Ref. 7). Campos, Méndez, and Fort[8] (CMF) were the first to derive a diffusion equation for fractals that is compatible with (3) as well as (2). CMF also used their diffusion operator to obtain a more general version of the Fisher equation and hence an approximate expression for the speed of Fisher equation fronts[8,9] which, following their derivation and the condition on $f$ given in Ref. 10, is straightforward to generalize to the case of fronts governed by (1) to arrive at what we will refer to as

the CMF formula for front speed,

$$V = \frac{1}{d_{\min}} \left( \frac{4D_0 d_{\min} f(0)}{d_w - d_{\min}} \right)^{\delta} t^{d_{\min}^{-1}-1}, \qquad (4)$$

where $D_0$, the fractal diffusion coefficient, is related to the proportionality constant in (2) via [11]

$$C = \frac{\Gamma[(d_f+2)\delta]}{\Gamma[d_f\delta]} \left( \frac{4D_0}{d_w \delta} \right)^{2\delta}, \qquad (5)$$

where $\Gamma(x)$ denotes the gamma function of $x$. For $d$-dimensional Euclidean space, $d_f = d$, $d_w = 2$, $d_{\min} = 1$, and $C = 2dD$ which leads to, in this case, $D_0 = D$ and (4) reduces to $V = 2\sqrt{f(0)D}$, a result which is well known for the Fisher equation [3].

The only fractals for which it has so far been possible to determine $d_w$ analytically are finitely ramified. A fractal is finitely ramified if any proper subset of it can be separated from the rest by removing a finite number of points. If a fractal is not finitely ramified, it is referred to as being infinitely ramified. In the case of finitely ramified loopless fractals with a topological dimension larger than 1, $d_w = d_f + 1$ [12]. For the simplest finitely ramified fractals with loops, such as the Sierpiński gasket, a closed-form expression for $d_w$ can be obtained using a renormalization procedure [7]. For more complicated finitely ramified fractals with loops, a renormalization procedure can be used to generate a set of equations from which $d_w$ can be found numerically [13]. Owing to the current lack of analytical approaches, numerical simulations of random walkers [14] or the exact enumeration of their distribution [15] on the lattice representation of the fractal are required to find $C$ in all cases and $d_w$ for infinitely ramified fractals.

The speed of simulated Fisher equation fronts on some finitely ramified fractals, namely, the Sierpiński gasket, the Koch curve, and a random fractal in the form of a percolation cluster near criticality, have been shown to agree quite well with (4) both in terms of time-dependence (the latter two fractals have $d_{\min} > 1$) and dependence on $f(0)$ [8,11]. Here we test the CMF formula for simulated fronts governed by (1) with $f(u) = a(1-u)(1-\alpha u)$ for $0 \leqslant \alpha \leqslant 1$ on a number of finitely ramified generalizations of the Sierpiński carpet along with the classic Sierpiński carpet and its random version which are both infinitely ramified. Such fractals are of interest since some fractals in nature, such as porous rock with a scale-invariant distribution of holes [16], are infinitely ramified.

Cubic reaction terms are used in a number of simplified models of reaction-diffusion systems [2,4]. The particular form of $f(u)$ was chosen as it reduces to the Fisher equation when $\alpha = 0$ and for all $\alpha \in [0,1]$, a long way ahead of (behind) the front $u$ tends to 0 (1). (The front is the set of points where $u = \frac{1}{2}$.) The asymmetry of $u_e(x)$, the monotonically decreasing stable equilibrium travelling waveform in an infinite domain with a phase chosen so that $u_e(0) = \frac{1}{2}$, increases with $\alpha$. The Fisher equation waveform is symmetrical in the sense that $u_e(x) - \frac{1}{2}$ is an odd function of $x$. For $\alpha \in (0,1]$, $u_e(x) \to 0$ for $x > 0$ more rapidly than $u_e(x) \to 1$ for $x < 0$, and this becomes more pronounced as $\alpha$ increases. In all cases, the width of the transition region around the front scales as $\sqrt{D/a}$.

For all generalized Sierpiński carpets, $d_{\min}$ is unity [17], and so, for the form of $f(u)$ we consider, (4) reduces to

$$V = Ka^{\delta} \qquad (6)$$

where now $\delta \equiv 1 - 1/d_w$ and

$$K \equiv \sqrt{\frac{C\Gamma[d_f\delta]}{\Gamma[(d_f+2)\delta]}}. \qquad (7)$$

In the next section we review some properties of generalized carpets and introduce a scheme for naming them. We then describe the technique used to obtain estimates of $C$ and $d_w$ (where they are not already known) and the simulation of the reaction-diffusion equation on the fractal lattices. A comparison of the speed of the simulated fronts with that predicted by the CMF formula follows, along with a discussion of the results.

## GENERALIZED SIERPIŃSKI CARPETS

A non-random generalized $N \times N$ Sierpiński carpet is constructed by starting from a filled square with sides of length $L$ which is divided into $N^2$ equal subsquares of length $L/N$, and then $q$ of these subsquares are removed. The remaining shape is known as the generator. The process is applied recursively: at the $m$th iteration each of the filled squares (of length $L/N^{m-1}$) is replaced by a copy of the generator scaled down by a factor of $N^{m-1}$ to give what is sometimes referred to as the prefractal of depth $m$. Thus the generator itself is the prefractal of depth 1 and the fractal is the prefractal of infinite depth. The fractal dimension of the resulting carpet is $\log_N(N^2 - q)$.

We introduce the following convention for naming the non-random generalized $N \times N$ carpets. We represent each filled (empty) subsquare in the generator by the binary digit 1 (0). The $N$ binary digits making up the representation of each row of the

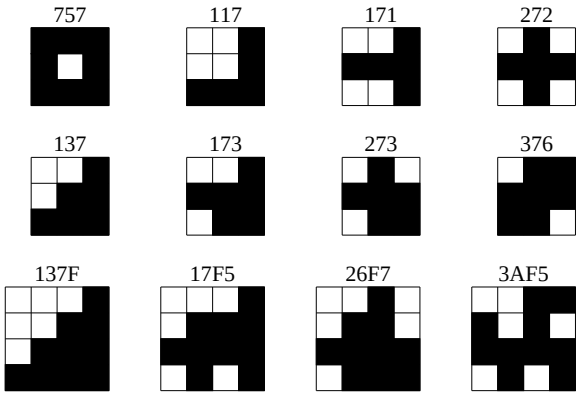


**Fig. 1** Generators of various generalized Sierpiński carpets with the names of the corresponding fractal carpets.

generator are replaced by their base-$2^N$ equivalent digit. This results in an $N$-digit base-$2^N$ number of which the $p$th most significant digit represents the $p$th row of the generator (counting from top to bottom). Thus according to this convention the classic $3\times3$ Sierpiński carpet is called 757. Rotating or reflecting a generator will result in the same fractal but in general a different $N$-digit code. To avoid duplication, we use the code corresponding to the orientation of the generator which gives the code with the lowest numerical value. Examples are given in Fig. 1.

A fractal carpet is finitely ramified if and only if the first and the last row of the generator have exactly one filled subsquare in the same position in the row and similarly for the first and last column[12]. Thus all carpets produced from the generators shown in Fig. 1 are finitely ramified except for the classic Sierpiński carpet, 757. Of the carpets shown, only 117, 171, 272, and 3AF5 are loopless.

Random generalized Sierpiński carpets specified by the parameters $N$ and $q$ can be constructed in a similar way to the non-random carpets except that each time a filled square is replaced by a generator, the generator used is picked uniformly at random from the set of the $\binom{N^2}{q}$ possible generators with $q$ empty squares. This results in a carpet with the same $d_\mathrm{f}$ as for the non-random case[7].

## NUMERICAL METHODS

The random walk simulations used to find $C$ and $d_\mathrm{w}$, and those used for the reaction-diffusion equation, are performed on a prefractal lattice. To obtain a prefractal lattice for a carpet, we place the prefractal whose smallest subsquares are unit squares on the first quadrant of a square lattice with unit spacing between lattice sites. In other words, the underlying lattice is composed of the points $(x,y)$ where $x,y\in\{0,1,2,\ldots\}$. The carpet is aligned so that the centres of the smallest subsquares are lattice points. The prefractal lattice is composed of all lattice points that are inside the prefractal.

Before describing the simulations, we present a way of finding whether a set of coordinates corresponds to a point on a given non-random prefractal carpet lattice. It is basically the same idea as the infinite lattice method[18] but we formulate it another way.

### Determining whether a point lies on the prefractal lattice

By way of introduction, consider the classic middle-third Cantor subset of the unit interval. It is well known that this consists of all points which can be written in base 3 in such a way that they do not contain the digit 1. In practice this means writing the end point 1 of the interval [0,1] as $0.\dot{2}$ and replacing a trailing 1 in a number by $0\dot{2}$. For example, the base-3 representation of $\frac{1}{3}$ is 0.1 which has a trailing 1 and thus may also be written as $0.0\dot{2}$, hence implying that it is in the subset. Similarly, the 757 carpet subset of the unit square $[0,1]\times[0,1]$ consists of all points $(x,y)$ such that, when $x$ and $y$ are written using the no-trailing-1 base-3 representation, there is no $m$ such that the $m$th digits of $x$ and $y$ are both 1.

Now consider the generator of an $N\times N$ generalized carpet where each subsquare is labelled by integer coordinates $(X,Y)$ where $X,Y\in\{0,1,\ldots,N-1\}$ and the bottom left subsquare is taken as the origin $(0,0)$. Let $Q$ be the set of coordinates of the empty subsquares of the generator. Then the corresponding generalized carpet subset of the unit square is the set of points $(x,y)$ such that when written in base $N$, there is no $m$ such that the ordered pair formed from the $m$th digits of $x$ and $y$ is in the set $Q$. In the case of the 757 carpet, $Q=\{(1,1)\}$.

To determine whether or not a point in the underlying lattice is in the depth-$M$ prefractal lattice of an $N\times N$ generalized carpet we use a procedure analogous to the one for determining whether or not a point in the unit square is in the generalized carpet. Let $S_m^{(N)}(x)$ be the $m$th digit of integer $x$ written in base $N$, counting the rightmost digit as the first. A point $(x,y)$ on the underlying lattice is not on the prefractal lattice if and only if there is an $m$ where $1\leqslant m\leqslant M$ such that $(S_m^{(N)}(x),S_m^{(N)}(y))\in Q$. The method can clearly be generalized to three (or more) dimensions.

**Finding $C$ and $d_w$**

We used a Monte-Carlo approach based on that in Ref. 19 to determine $C$ and $d_w$. We released $2^{15}$ walkers distributed at random onto a depth-$M$ prefractal lattice. For the non-random carpets, rather than have an array describing the lattice, we used the algorithm described above to determine whether a site is on the prefractal. This enabled us to use $M = 15$ (the limit set by the size of the largest integer possible for the variable type used in the program). Having a large depth ensures that only a small fraction of walkers feel the effect of the boundary[19]. For the $3 \times 3$ random carpet with $q = 1$ (which we will refer to as R), we used $M = 10$. The walkers move according to the blind ant algorithm whereby at each time step, one of the walker's four neighbouring sites on the underlying lattice is chosen at random. The walker only moves there if it coincides with the prefractal lattice.

$\langle r^2 \rangle$ against $t$ is plotted logarithmically for integer values of $t$ nearest to $2^{j/8}$ for $j = 56, \ldots, j_{\max}$ with $j_{\max}$ generally at least 144. Values of $C$ and $d_w$ obtained from the best-fit line vary with $j_{\max}$. For carpets whose $d_w$ value is already known accurately, we selected the $j_{\max}$ which gave the closest $d_w$ to the known value and then used the corresponding value of $C$.

**Reaction-diffusion fronts on carpets**

Our numerical scheme for solving (1) with $D = 1/2d$ on a prefractal carpet lattice is based on the method given in Ref. 20. The following system of equations was solved using the 4th-order Runge-Kutta method:

$$\frac{\mathrm{d}u_i}{\mathrm{d}t} = \frac{\left(\sum_{j=1}^{p_i} u_{ij}\right) - p_i u_i}{2d} + u_i f(u_i), \qquad (8)$$

where $u_i$ and $u_{ij}$ are the values of $u$ at the $i$th node and at the $j$th nearest neighbour of the $i$th node, respectively, and $p_i$ is the number of nearest neighbours of the $i$th node. A time step of 1 was used. The prefractal lattices used were of depths 6 and 5 for the $3 \times 3$ and $4 \times 4$ carpets, respectively.

We employed two types of boundary conditions. In type O, a single node is held fixed at a value of 1 for all time. Except for the 272 carpet in which case the fixed node is at the centre of the prefractal, the fixed node was the origin. The prefractal lattice thus had to be oriented so that its corner node coincided with the origin. In type L, all the nodes in the prefractal lattice along the $y$-axis had $u = 1$ for all time. At all other points, the initial value of $u$ is set equal to 0. Note that at the edge of the lattice, the scheme (8) naturally results in free boundary conditions. On a 2-d Euclidean lattice using boundary conditions of type O (L), a circular (planar) wave (of the form $u_e(r - Vt - r_0)$ where $r$ is the distance measured in the direction of propagation and $r_0$ is a phase constant) develops after some time.

The front itself was taken as the set of points with $u \leqslant \frac{1}{2}$ which had at least one neighbouring node with $u \geqslant \frac{1}{2}$. For type O boundary conditions, the mean front distance $F$ was found from the mean distance of the front points from the fixed-valued node. For type L boundary conditions, $F$ was taken to be the mean $x$ coordinate of the front points. The distance of the front points furthest from the origin or $y$-axis was also monitored. When this reached 0.8 of the width of the prefractal, the simulation was halted to avoid the wavefront feeling the effects of the boundary. The mean front speed $V_{\mathrm{sim}}$ was obtained from a best-fit line of $F$ plotted against $t$, discarding the points before the waveforms have had time to fully develop.

The scheme gives fronts with a speed within 3% of the theoretical value for $0.0025 < a < 0.16$ on a 1-d lattice. This, in addition to the fact that no oscillations were seen in any of the simulations, suggests that the scheme was not subject to numerical instabilities. Simulations were carried out for $a = 0.16/2^s$ with $s = 0, 1, \ldots, 7$ and $\alpha = 0, 0.9, 1$ on the carpets whose generators are given in Fig. 1 along with the random carpet R. Boundary conditions of type O were used for all carpets. For 757 and R we also ran simulations with the type L boundary.

## RESULTS AND DISCUSSION

The values of $C$ we obtained are given in Table 1. We have not managed to find any other values of this parameter in the literature to compare them with. From the variations in the values of $C$ obtained from the best-fit lines as $j_{\max}$ is varied, we estimate that the uncertainty in $C$ is less than 1%. Hence the uncertainty in $K$ is less than 0.5% for the carpets whose $d_w$ is known accurately.

For the 757 carpet, $d_w = 2.10$ is in line with the result of $2.101 \pm 0.022$ reported in Ref. 21. Our error bounds would be no more than $\pm 0.01$. For the particular instance of the random carpet we used (Fig. 2), the $d_w$ value of 2.175 we obtain is a little outside the range of $2.13 \pm 0.03$ suggested in Ref. 22. There were problems with finding $C$ for 3AF5 as the $d_w$ value quickly converged to 2.72 with increasing $j_{\max}$. This is 0.06 larger than the theoretical value and it is interesting that this is close to the central

**Table 1** Parameters for the carpets studied and a comparison of the simulation results with the CMF formula. $[\rho_\alpha]$ denotes the range of values of $\rho$ obtained for the various values of $a$ used for a particular value of $\alpha$. Thus $[\rho_0]$ gives the range of relative discrepancy for Fisher equation fronts. $\mu_s \equiv V_{\rm sim}(0.16/2^s,1)/V_{\rm sim}(0.16/2^s,0)-1$.

| carpet | $C$ | $d_{\rm w}$ | $K$ | $\delta$ | $[\rho_0]$ | $[\rho_{0.9}]$ | $[\rho_1]$ | $\mu_7$ | $\mu_0$ |
|---|---|---|---|---|---|---|---|---|---|
| 757 | 0.792 | 2.10 | 0.885 | 0.524 | [−0.03,0.02][e] | [−0.04,0.02][e] | [−0.04,0.02][e] | 0.00 | 0.00 |
| | | | | | [−0.03,0.02][e] | [−0.03,0.03][e] | [−0.03,0.03][e] | 0.00 | 0.00 |
| 117 | 0.636 | 2.4650[a] | 0.823 | 0.594 | [0.14,0.16] | [0.14,0.16] | [0.14,0.16] | 0.00 | 0.00 |
| 171 | 0.615 | 2.4650[a] | 0.809 | 0.594 | [0.14,0.19][e] | [0.14,0.17] | [0.14,0.18] | −0.01 | −0.03 |
| 272 | 0.598 | 2.4650[a] | 0.798 | 0.594 | [0.07,0.10] | [−0.01,0.13] | [0.00,0.13] | 0.02 | 0.00 |
| 137 | 0.704 | 2.5448(9)[b] | 0.801 | 0.607 | [0.04,0.08] | [0.00,0.10] | [0.03,0.06] | 0.00 | −0.01 |
| 173 | 0.698 | 2.5448(4)[b] | 0.797 | 0.607 | [0.09,0.14] | [0.09,0.12][e] | [0.09,0.12][e] | 0.00 | 0.00 |
| 273 | 0.689 | 2.5448(4)[b] | 0.792 | 0.607 | [−0.22,−0.18][e] | [−0.22,−0.18] | [−0.22,−0.20] | 0.07 | 0.00 |
| 376 | 0.740 | 2.5427(7)[b] | 0.784 | 0.607 | [−0.25,−0.19][e] | [−0.25,−0.21][e] | [−0.25,−0.21][e] | 0.00 | −0.02 |
| 137F | 0.765 | 2.5094(3)[b] | 0.833 | 0.601 | [−0.03,0.04] | [−0.01,0.04] | [−0.02,0.02] | 0.00 | −0.03 |
| 17F5 | 0.746 | 2.5758(7)[b] | 0.810 | 0.612 | [0.02,0.09] | [0.01,0.08] | [0.01,0.08] | −0.01 | 0.00 |
| 26F7 | 0.740 | 2.4915(5)[b] | 0.823 | 0.599 | [−0.04,−0.01] | [−0.04,−0.02] | [−0.04,−0.02] | 0.00 | 0.00 |
| 3AF5 | 0.566 | 2.6609[a] | 0.693 | 0.624 | [−0.37,−0.33][e] | [−0.33,−0.37][e] | [−0.33,−0.37][e] | 0.00 | 0.00 |
| R | 0.849 | 2.175 | 0.894 | 0.540 | [−0.05,−0.03][e] | [−0.05,−0.02][e] | [−0.05,−0.02][e] | 0.00 | 0.00 |
| | | | | | [−0.02,0.00][e] | [−0.02,0.00][e] | [−0.02,0.00][e] | 0.00 | 0.00 |

Where two intervals for $\rho$ are given, the first and second are for boundary conditions of type O and L, respectively.
[a] From $d_{\rm w} = 1 + d_{\rm f}$ for loopless carpets.
[b] Values from resistance scaling calculation in Ref. 13. The number in brackets indicates the uncertainty in the final decimal place.
[e] $[A,B]^{\rm e}$ denotes that $\rho_\alpha(0.16/2^7) = A$, $\rho_\alpha(0.16) = B$, and $\rho_\alpha(a) \in [A,B]$ for $0.16/2^7 < a < 0.16$.

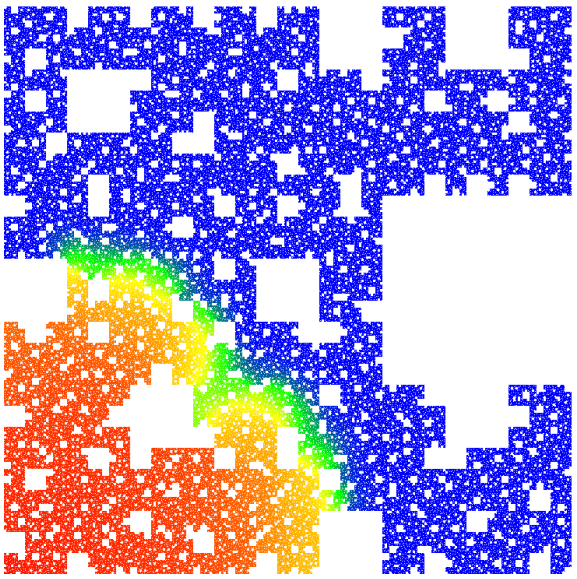

**Fig. 2** Reaction-diffusion equation simulation on a random carpet for $\alpha = 1$, $a = 0.0025$ at time $t = 14000$. Type O boundary. Red: $u = 1$; yellow: $u = 0.5$; blue: $u = 0$.

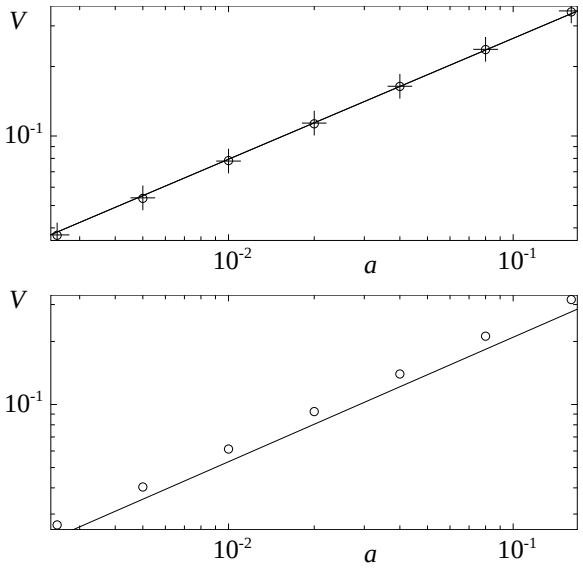


**Fig. 3** Simulation results for 757 (top) and 117 (bottom) carpets with $\alpha = 0$. Circles: type O boundary; crosses: type L boundary; solid line: CMF formula.

value of 2.71±0.05 arrived at via exact enumeration in Ref. 14. We ended up using a $j_{\rm max}$ of just 25 in order to obtain a value of $d_{\rm w}$ reasonably close to the theoretical value. The corresponding estimate of $C$ therefore has a greater uncertainty than for the other carpets.

We use $\rho_\alpha(a) \equiv V_{\rm sim}(a,\alpha)/Ka^\delta - 1$ to measure

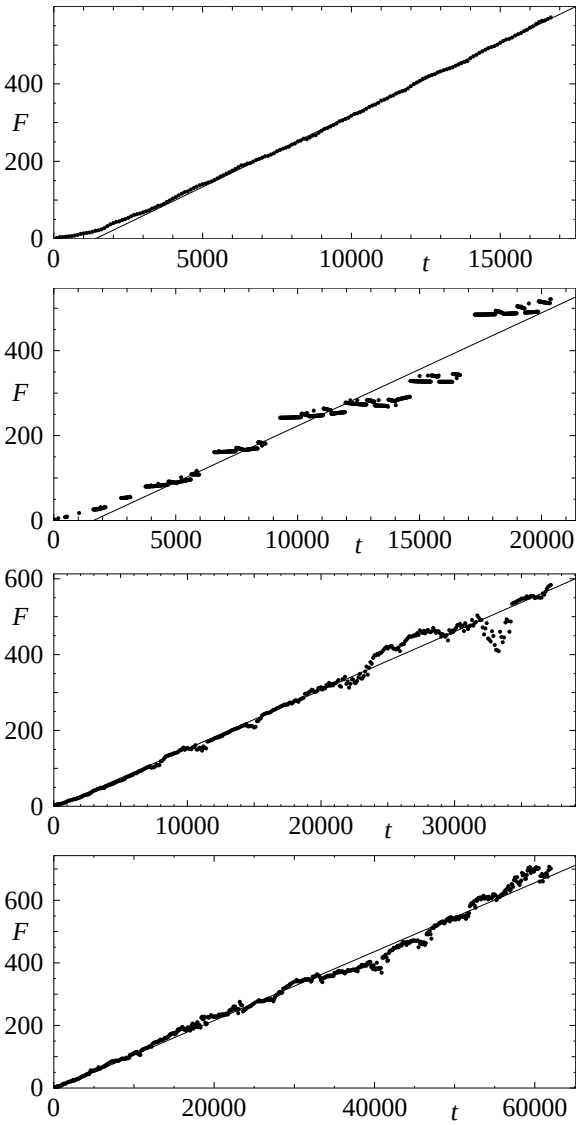


**Fig. 4** $(t, F)$ plots for 757, 117, 376, 3AF5 (from top to bottom) with $a = 0.0025$ and $\alpha = 0$. The best-fit line (which does not use the points for $t < 5000$) is used to calculate the mean front speed.

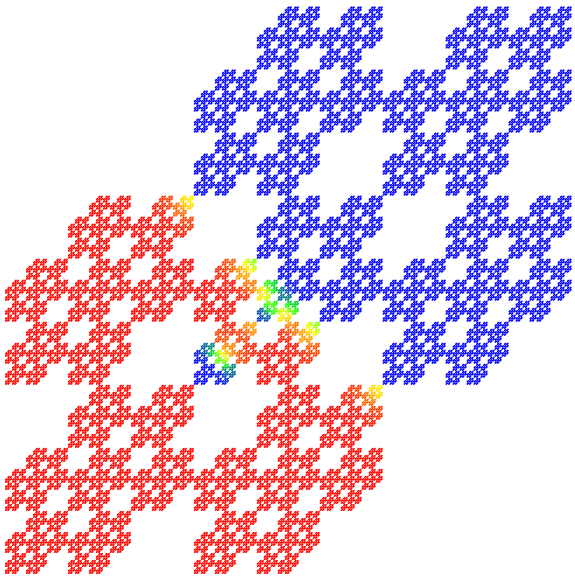

**Fig. 5** Reaction-diffusion equation simulation on the 376 carpet for $\alpha = 0$, $a = 0.0025$ at time $t = 32000$.

the sign and magnitude of the discrepancy between the simulation result of the mean front speed $V_{\text{sim}}(a, \alpha)$ and that predicted by the CMF formula (6). Based on the estimated errors of the front velocity in a homogeneous medium and the values of $K$, we take values of $|\rho|$ of less than around 0.04 as agreeing well with the CMF formula. Table 1 (and Fig. 3 for 757) show that there is agreement with the CMF formula for the infinitely ramified carpets (757 and R) and some of the $4 \times 4$ carpets with loops, namely, 137F and 26F7. There was no significant difference between the results found for the type O and L boundary conditions.

The agreement is less good for the loopless carpets along with some of the others (Table 1, Fig. 3). This is perhaps due to the more erratic behaviour of the mean front distance $F$ against $t$ in such cases when compared to infinitely ramified fractals (Fig. 4). For loopless carpets, a sudden jump in $F$ will occur when the front disappears when it reaches the end of a branch. Loopless fractals are not the only type of fractal that have dead ends, as is illustrated in Fig. 5. It can be seen that the drop in $F$ around $t = 32000$ (Fig. 4) results from some fronts propagating towards the origin. Shortly after, all fronts disappear except for the one right at the centre which marks the only link from one half of the fractal to the other. And occurring on a fractal, this phenomenon is found on all scales at various other times. In spite of the irregular nature of the $(t, F)$ plots, the points in Fig. 3 for 117 lie in a straight line (as is also the case for the other carpets) which indicates that our calculation of $V_{\text{sim}}$ is consistent. It is interesting to note that the carpet with the largest $|\rho_\alpha|$, namely, 3AF5, is the one for which finding $d_{\text{w}}$ was problematic.

The CMF formula does not involve $\alpha$. However, in some cases, there is an indication that $\alpha$ has an effect on the mean front speed (see $[\rho_\alpha]$ and $\mu_s$ values in Table 1). As this only occurs for some of the carpets which have erratic $(t, F)$ plots and

generally show poorer agreement with the CMF formula, it seems probable that this discrepancy has the same root cause. Note also that the precise nature of the $(t, F)$ plots varies with $\alpha$. This results from the shape of the wave $u_e(x)$ depending on $\alpha$ and so the time where the wavefront disappears in one part of the fractal (resulting in a jump in $F$) will be also affected by $\alpha$ even if the overall average front speed remains unchanged.

In summary, as the predictive tool CMF proposed their formula to be[11], it generally works quite well, although the cases where it fails to work so well are worthy of further investigation. It is pleasing that the fractals for which it gives the best agreement are the less obscure ones, such as the classic Sierpiński and random carpets, which are more reminiscent of the fractals found in nature. The results presented here give further credence to the formula being of use to experimentalists, as CMF suggested in the conclusion of Ref. 11.

*Acknowledgements*: Funding from the Thailand Research Fund (RGJ49) is gratefully acknowledged. OS and MAA thank the Department of Physics, University of Wisconsin for the use of its facilities during their visits and Kit Matan for the use of his computer. We also thank the four anonymous referees for their comments.

## REFERENCES

1. Gray P, Scott SK (1990) *Chemical Oscillations and Instabilities: Non-linear Chemical Kinetics*, Clarendon Press, Oxford.
2. Scott A (1999) *Nonlinear Science: Emergence and Dynamics of Coherent Structures*, Oxford Univ Press, Oxford.
3. Fisher RA (1937) The wave of advance of advantageous genes. *Ann Eugen* **7**, 355–69.
4. Murray JD (2002) *Mathematical Biology*, 3rd edn, Springer, New York.
5. Mandelbrot BB (1982) *The Fractal Geometry of Nature*, W. H. Freeman, New York.
6. Mosco U (1997) Invariant field metrics and dynamical scalings on fractals. *Phys Rev Lett* **79**, 4067–70.
7. ben Avraham D, Havlin S (2000) *Diffusion and Reactions in Fractals and Disordered Systems*, Cambridge Univ Press, Cambridge.
8. Campos D, Méndez V, Fort J (2004) Description of diffusive and propagative behavior on fractals. *Phys Rev E* **69**, 031115.
9. Méndez V, Campos D, Fort J (2004) Dynamical features of reaction-diffusion fronts in fractals. *Phys Rev E* **69**, 016613.
10. Fedotov S, Méndez V (2002) Continuous-time random walks and traveling fronts. *Phys Rev E* **66**, 030102(R).
11. Campos D, Fort J, Méndez V (2004) Propagation through fractal media: The Sierpinski gasket and the Koch curve. *Europhys Lett* **68**, 769–75.
12. Havlin S, Ben-Avraham D (1987) Diffusion in disordered media. *Adv Phys* **36**, 695–798.
13. Schulzky C, Franz A, Hoffmann KH (2000) Resistance scaling and random walk dimensions for finitely ramified Sierpinski carpets. *ACM SIGSAM Bull* **34**, 1–8.
14. Franz A, Schulzky C, Anh DHN, Seeger S, Balg J, Hoffmann KH (2006) Random walks on fractals. In: Hoffmann KH, Meyer A (eds) *Parallel Algorithms and Cluster Computing: Implementations, Algorithms and Applications*, Springer, Berlin, pp 303–13.
15. Majid I, Ben-Avraham D, Havlin S, Stanley HE (1984) Exact-enumeration approach to random walks on percolation clusters in two dimensions. *Phys Rev B* **30**, 1626–8.
16. Giménez D, Perfect E, Rawls WJ, Pachepsky Ya (1997) Fractal models for predicting soil hydraulic properties: a review. *Eng Geol* **48**, 161–83.
17. Bunde A, Havlin S (1994) A brief introduction to fractal geometry. In: Bunde A, Havlin S (eds) *Fractals in Science*, Springer-Verlag, pp 1–26.
18. Dasgupta R, Ballabh TK, Tarafdar S (1999) Scaling exponents for random walks on Sierpinski carpets and number of distinct sites visited: a new algorithm for infinite fractal lattices. *J Phys A* **32**, 6503–16.
19. Anh DHN, Hoffmann KH, Seeger S, Tarafdar S (2005) Diffusion in disordered fractals. *Europhys Lett* **70**, 109–15.
20. Bianco F, Chibbaro S, Vergni D, Vulpiani A (2013) Reaction spreading on percolating clusters. *Phys Rev E* **87**, 062811.
21. Aarão Reis FDA (1995) Finite-size scaling for random walks on fractals. *J Phys A* **28**, 6277–88.
22. Aarão Reis FDA (1996) Diffusion on regular random fractals. *J Phys A* **29**, 7803–10.